# PERFORMANCE OF ALUMINUM NITRIDE CURVED PMUT ARRAYS FABRICATED USING GLASS BLOWING TECHNIQUE

Shubham P. Khandare<sup>1\*</sup>, Chichen Huang<sup>2\*</sup>, Sri-Rajasekhar Kothapalli<sup>1</sup>, and Srinivas Tadigadapa<sup>2</sup>

<sup>1</sup>The Pennsylvania State University, University Park, PA 16802 USA

<sup>2</sup>Northeastern University, Boston, MA 02115, USA

\*Authors contributed equally

## **ABSTRACT**

We present the initial characterization results of curved piezoelectric micromachined ultrasound transducer (pMUT) arrays fabricated using the chip-scale glassblowing method. The three-dimensional pMUTs are realized by depositing 750 nm thick 30% scandium-doped aluminum nitride (Sc-AlN) on curved suspended glass diaphragms of 150 µm diameter. Performance of a 13 × 13 row-column-addressable curved pMUT array, characterized using electrical impedance, Laser Doppler vibrometer (LDV), and hydrophone. The electrical impedance and LDV measurement showed the device resonance frequency of ~4.2 MHz in air, and the hydrophone measurement showed a resonance frequency of ~2.58 MHz in water. The DC response measured with LDV was 0.3 nm/V. The acoustic field profile obtained from hydrophone measurements showed a peak pressure of 0.4353 kPa/V/cell, at 7 mm, spatial-peak-temporal-average intensity  $I_{SPTA} = 476 \text{ mW/cm}^2$ , acoustic focal length of 4.27 mm, and focal width of 2.1 mm at 54.1  $V_{pp}$  electrical input.

#### **KEYWORDS**

Ultrasound transducers array, scandium-doped aluminum nitride, chip-scale glass blowing, curved glass structures, piezoelectric micromachined ultrasound transducer (pMUT)

## INTRODUCTION

Ultrasound vibrations ranging from 20 kHz to several GHz propagating through solids, liquids, and gases, are playing crucial roles in applications ranging from industrial non-destructive testing, consumer electronics and Internet of Things devices, to medical diagnosis and therapeutic treatment. The non-invasive nature and sub-mm scale spatial resolution even several centimeters deep inside the tissue [1] of ultrasound has proven to be effective in several pre-clinical and clinical applications such as medical imaging [2] and in treating neural disorders via neurostimulation and -modulation [3]. Based on the parameters such as spatial-peak-pulse-average intensity ( $I_{SPPA}$ ),  $I_{SPTA}$ , frequency, and period of ultrasound stimulation [1], these neuro-stimulation mechanisms are categorized into lowintensity focused ultrasound (LIFU) with  $I_{SPTA} < 20 \text{ W/cm}^2$ [4], and high-intensity focused ultrasound (HIFU) with  $I_{SPTA} > 20 \text{ W/cm}^2$  [4]. In recent decades, the sub-mm scale resolution of LIFU has captured the interest of researchers to explore its pre-clinical applications in animal models [5]. Bulk piezoelectric transducers in single-elements and arrays configurations [5], and MEMS-based capacitive micro-machined ultrasound transducers (cMUTs) [6], [7] were previously demonstrated for neuromodulation applications. Operating in plate flexural mode, cMUTs

offer compact size, economical batch fabrication, low costs, and flexibility in frequency ranges compared to conventional thickness mode transducers. Despite high electromechanical coupling factors, both bulk piezoelectric transducers and cMUTs require high excitation voltage for operations. The single-element bulk piezoelectric transducers used in LIFU stimulation applications have fixed focal zones and beam profiles, which reduces the targeting accuracy [1]. Whereas cMUTs suffer from high DC bias voltage, high parasitic effect, and limited deflection. diaphragm In contrast, piezoelectric micromachined ultrasound transducers (pMUTs) operate at lower voltages and lower impedance than cMUTs but have lower electromechanical coupling factors. Efforts have been made to improve pMUTs outputs by modifying diaphragm geometry and design configurations of electrodes. A two-port electrode design for pMUTs boosted acoustic output to 2x compared to single-port pMUTs [8]. Additionally, bimorph pMUTs with two active AlN layers achieved a 4x higher acoustic output than unimorph pMUTs of similar size [9]. However, bimorph transducers increase pressure output at the same frequency as their planar counterparts.

Recent studies showed that curved pMUTs can generate high-pressure output at higher frequencies, due to both in-plane stress and stress gradients, compared to the planar pMUTs of the same size which rely solely on stress gradients in the membrane layers for out-of-plane bending [10]-[12]. Given that the typical size of pMUTs ranges from 0.05 to 0.5 of the wavelengths, they function like a point source of ultrasound at the device surface. Whereas the inherent membrane curvature in curved transducers imparts self-mechanical focusing capabilities to these transducers. This focusing ability even extends to the micro-structure of curved pMUTs, creating micro-focal regions for all cells. These membrane micro-curvatures allow the device to produce its virtual point sources away from the device surface giving it a unique feature over planar pMUTs. Previous attempts at curving the cell involved coating wax mold with parylene - C to create curved zinc oxide-based pMUTs [13] are unsuitable for large-scale fabrication of arrays[11]. Thin film PZT-based curved pMUTs [14], despite having an electro-mechanical coupling factor of 45%, lack compatibility with CMOS processes [15] with a thermal budget of > 500 °C [16]. Curved pMUTs fabricated using CMOS-compatible techniques, involving wet isotropic etching of silicon and subsequent deposition of low-temperature oxide (LTO) and aluminum nitride (AlN) [10], result in underutilized wafer areas and yielding arrays with low fill-factor. To improve the fill factor of the curved pMUTs, researchers proposed curving the diaphragm using residual

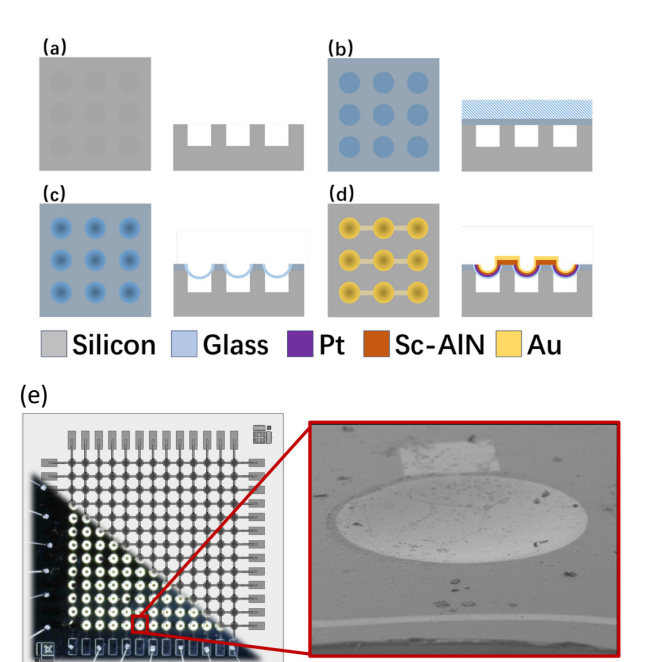


Figure 1: Process flow of proposed curved pMUT array. (a) patterning and etching the Si substrate, (b) anodic bonding glass and Si; thinning down the glass, (c) heating the chip and the spherical deformation due to the pressure difference between atmosphere and cavity vacuum, (d) depositing and patterning Pt/Sc-AlN/Au. (e) A picture of a fabricated 13 × 13 element row-column addressable (RCA) curved pMUT array and a zoomed picture on the right show a scanning electron microscope image of a single curved pMUT cell. Si: Silicon, Pt: Platinum, Sc-AlN: Scandium-doped Aluminum Nitride, Au: Gold

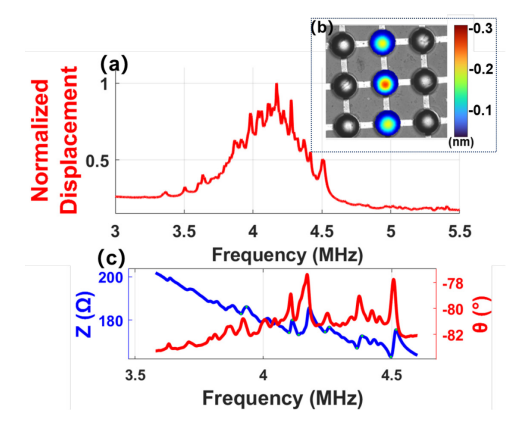


Figure 2: LDV measurement of the fabricated PMUT array: (a) normalized displacement of all the scan area of all cells excited by chirp signal, (b) A picture of offresonant measurement at 200kHz (c) measured frequency response in air using an electrical impedance analyzer.

stresses in the film [11]. However, the materials available for fine-tuning the residual stresses are limited and the static diaphragm deflection obtained through this method was around 2.5 µm [11]. Analytical studies have shown that a diaphragm with higher curvature gives greater acoustic output [12], [17]. Recently, the technique of the chip-scale glass blowing to fabricate curved pMUTs [12]

has been shown to allow precise control over membrane curvature without any constraints imposed by previous fabrication techniques, with additional advantages such as CMOS compatibility and high fill factor with efficient use of wafer real estate. It has been demonstrated that the technique is capable of fabricating curved pMUTs with diameters varying from 75 to 750 µm with curvature depth ranging from 0.2 to 76 µm [12]. In this work, we will present the fabrication of a 13 × 13 element row-column addressable (RCA) curved pMUT array, with each element in the array consisting of single curved pMUT diaphragms of 150 µm diameter, using the glass-blowing technique. The mode vibrations, resonance frequency, and pressure field of the curved pMUT array were characterized using electrical impedance, LDV, and hydrophone measurements.

## **FABRICATION**

#### **Process Flow**

The fabrication process flow for the  $13 \times 13$  element RCA curved pMUT array is shown in Fig. 1. Fig. 1 (a-d) show the schematics of the fabrication process from wafer to final device as reported in the reference [12], and Fig. 1 (e) shows a picture of the fabricated  $13 \times 13$  element RCA curved pMUT array and scanning electron microscope image of a single curved pMUT cell in the array. The design specifications of the fabricated  $13 \times 13$  element RCA curved pMUT array are listed in Table 1.

Table 1: Design specifications of single curved PMUT cell of 13x13 array

	Design Specifications (μm)			
Device Layer	Diameter size	Thickness	Depth of Curvature	
Glass Membrane		5		
30% Sc-AlN		0.75		
Ti/Pt Bottom Electrode	150	0.020/0.1	10-13	
Cr/Au Top Electrode		0.020/0.1		
Silicon Substrate	-	500	-	

# **RESULTS AND DISCUSSION**

Electrical impedance and LDV characterizations of individual elements of the curved pMUT array were performed in the frequency range of 3 to 5.5 MHz in air. The LDV measurement of the curved pMUT cells in Fig. 2(a) shows the average displacement of the scan area of all cells excited by the chirp signal. The center frequency in air was measured ~4.2 MHz. The off-resonant displacement at 200 kHz was around 0.2~0.3 nm/V as shown in Fig. 2(b). The highest  $k^2_{\rm eff}$ , calculated from impedance measurements in Fig. 2(c), was found to be 2%. Subsequently, the array was coated with parylene-C polymer for acoustic pressure characterization in water. The resonant frequency of the planar pMUT cell immersed in the water was reported as [18],

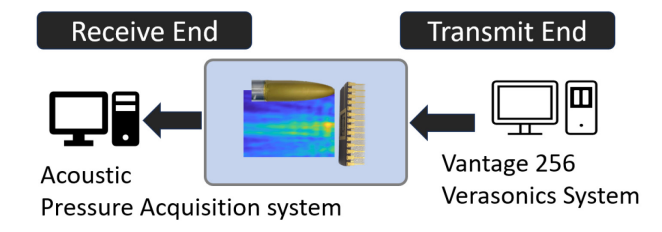


Figure 3. The schematic of transmit acoustic pressure characterization of the  $13 \times 13$  element curved pMUT array using a hydrophone and the Vantage 256 ultrasound data acquisition system.

$$f_{0,fluid} \approx \frac{f_{0,air}}{\sqrt{1+0.34 \frac{\rho_{fluid}d}{\mu}}}$$

Where,  $\mu = \sum_{i=1}^{n} \rho_i t_i$ ,  $\rho_i$  is the density of layer in pMUT membrane,  $t_i$  thickness of the layer in pMUT membrane,  $\rho_{fluid}$  is density of the fluid, and d diameter of the membrane. The  $f_{0.fluid}$  is predicted to be around 1.5 to 2.97 MHz. The COMSOL simulation (COMSOL Multiphysics, Burlington, MA, USA) predicted the frequency of 2.89 MHz with a curved pMUT cell model immersed in the water medium. The experimental setup as shown in Fig. 3 was used to characterize the 13 × 13 element curved pMUT array in row-addressable configuration. All the 13 column electrodes were shorted to trigger the array in row addressable configuration. Therefore the device functioned as a 13-element linear array with 13 cells in an individual element. For initial measurements, the curved pMUT array was excited with a phase-delayed impulse input from a Vantage 256 ultrasound system (Versonics Inc., Kirkland, WA, USA) with 2-cycles of sine-wave, 30 Vpp, at a frequency 2.89 MHz as predicted by the COMSOL model. The capsule hydrophone (ONDA HGL-080, Sunnyvale, CA, USA) was used to measure the acoustic pressure Aline near the focal zone, as depicted in Fig. 4. The initial hydrophone measurements showed a center frequency of

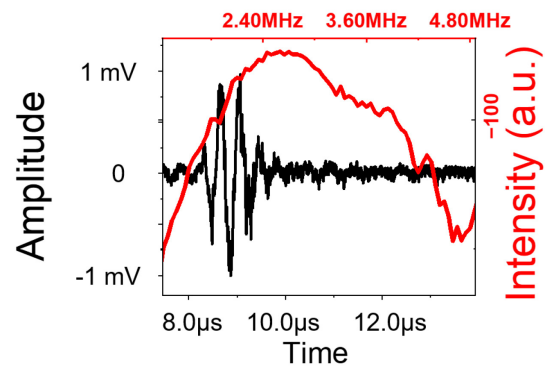


Figure 4: Hydrophone measured acoustic pressure A-line of the  $13 \times 13$  curved pMUT array at 2.9 MHz with  $30 V_{pp}$  at  $8 \mu s$  (12 mm) distance with phased array beamforming measured using hydrophone.

2.58 MHz for the curved pMUT array cells, determined from the Fast-Fourier Transform (FFT) of the A-line signal received at a 12 mm distance (~8 μs). The deviation in the analytical, simulated, and experimental values of resonant frequency can be attributed to the discrete and imperfect cells in elements and the assumption of continuous and perfect cells and elements in the array. In subsequent measurements, the electrical pulses of 2 cycles of sine-

wave input were applied at the experimentally measured center frequency (2.58 MHz) in water, and 54.1  $V_{pp}$  to the curved pMUT array, while the elements of the array were electronically steered to focus at ~7 mm away from the array. The acoustic pressure profile (A-line) of the array was measured with the hydrophone at each scan position in the XZ plane.

Pressure in Azimuthal-Longitudinal Plan of the transducer

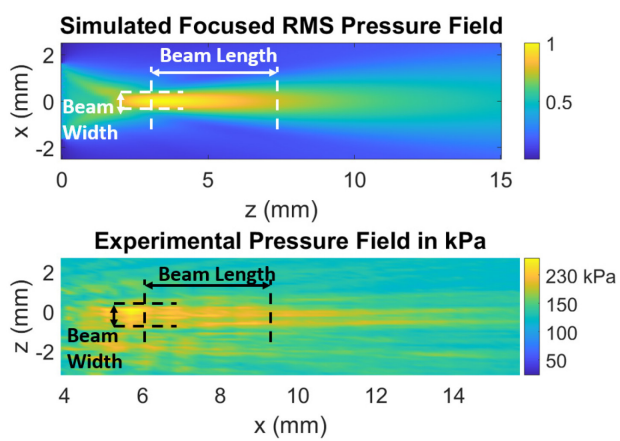


Figure 5: Acoustic pressure map in XZ plane of the 13×13 element curved pMUT array driven with a 54.1 Vpp, 2 cycles, 2.58 MHz sine wave pulse. Top: Simulation and Bottom: Experimental Pressure profiles.

Table 2: Comparison of acoustic pressure output of different pMUT array devices.

Material  $f_0$  (MHz) d (mm)  $m \times n$   $P_n$  (kPa/V/n

Material	$f_{\theta}$ (MHz)	d (mm)	$m \times n$	$P_n$ (kPa/V/mm <sup>2</sup> )			
AIN[19]	9	1.5	8 x 8	0.34			
15% Sc-AIN[19]	9	1.5	7 x 7	1.4			
AIN[20]	22	1.2	24 x 8	1.24			
AIN[21]	18.6	1	1261	7.5781			
PZT[22]	0.430	1	1 x 16	0.288			
PZT[23]	1.4	20	1 x 32	0.146			
30% Sc-AIN [This work]	2.58	7.0	13 x 13	0.4353			
$f_{\theta}$ = frequency, $d$ = distance from the device, $m \times n$ = array size, $Pn$ = Normalized Pressure Output							

Fig. 5 shows the acoustic pressure field from the 13-element array measured using simulation and experiments. The experimentally measured value of normalized acoustic pressure of  $0.4284~\text{kPa/V/mm}^2$ , normalized acoustic intensity of  $0.2082~\text{mW/cm}^2/\text{V/cell}$ ,  $I_{SPTA}=476~\text{mW/cm}^2$  and mechanical index, MI =  $0.0745~\text{at}~54.1~\text{V}_{pp}$  in water at a distance of  $\sim 6~\text{mm}$  transmit focus compares well with previously reported pMUTs in Table 2 where the focus was much closer to the device. The acoustic pressure field distribution of the transducer showed 2.1 mm of focal width and 4.27 mm of focal length.

# **CONCLUSION**

A curved pMUT array of row-column addressable configurations was fabricated and characterized to assess its performance for neuromodulation applications. The pMUTs are realized on curved suspended glass membranes

using the chip-scale glass-blowing method with 30%Sc-AlN as the piezoelectric material to improve devices. The acoustic peak pressure was comparable to previously reported AlN and PZT pMUTs. Since the development is relatively new we expect further improvements in the performance of acoustic pressure focus with optimal cell diameter, excitation parameters, and an increase in the number of elements in the array and generating sufficient acoustic pressure intensity for neuromodulation without craniotomy.

## **ACKNOWLEDGEMENTS**

This work was supported by the National Science Foundation (NSF) under Grant 2053591.

## REFERENCES

- [1] H. S. Gougheri, A. Dangi, S.-R. Kothapalli, and M. Kiani, "A comprehensive study of ultrasound transducer characteristics in microscopic ultrasound neuromodulation," *IEEE Trans Biomed Circuits Syst*, vol. 13, no. 5, pp. 835–847, 2019.
- [2] L. G. Montilla, R. Olafsson, D. R. Bauer, and R. S. Witte, "Real-time photoacoustic and ultrasound imaging: A simple solution for clinical ultrasound systems with linear arrays," *Phys Med Biol*, vol. 58, no. 1, Jan. 2013.
- [3] Y. Jo, C. Oh, and H. J. Lee, "Microelectromechanical systems-based neurotools for non-invasive ultrasound brain stimulation," *Chronobiology in Medicine*, vol. 1, no. 2, pp. 55–59, 2019.
- [4] J. Dell'Italia, J. L. Sanguinetti, M. M. Monti, A. Bystritsky, and N. Reggente, "Current State of Potential Mechanisms Supporting Low Intensity Focused Ultrasound for Neuromodulation," Front Hum Neurosci, vol. 16, p. 872639, Apr. 2022.
- [5] E. Rezayat and I. G. Toostani, "A Review on Brain Stimulation Using Low Intensity Focused Ultrasound," *Basic Clin Neurosci*, vol. 7, no. 3, p. 187, 2016.
- [6] P. Tipsawat, S. J. Ilham, J. I. Yang, Z. Kashani, M. Kiani, and S. Trolier-Mckinstry, "32 element piezoelectric micromachined ultrasound transducer (PMUTs) phased array for neuromodulation," *IEEE open journal of ultrasonics, ferroelectrics*, and frequency control, vol. 2, pp. 184–193, 2022.
- [7] C. Seok, O. J. Adelegan, A. O. Biliroglu, F. Y. Yamaner, and O. Oralkan, "A Wearable Ultrasonic Neurostimulator Part II: A 2D CMUT Phased Array System with a Flip-Chip Bonded ASIC," *IEEE Trans Biomed Circuits Syst*, vol. 15, no. 4, pp. 705–718, Aug. 2021.
- [8] H. Kim et al., "Miniature ultrasound ring array transducers for transcranial ultrasound neuromodulation of freely-moving small animals," *Brain Stimul*, vol. 12, no. 2, pp. 251–255, Mar. 2019.
- [9] F. Sammoura, S. Shelton, S. Akhbari, D. Horsley, and L. Lin, "A two-port piezoelectric micromachined ultrasonic transducer," in *Joint IEEE International Symposium on the Applications of Ferroelectric, International Workshop on Acoustic Transduction Materials and Devices & Workshop on Piezoresponse Force Microscopy*, 2014, pp. 1–4.
- [10] S. Akhbari, F. Sammoura, C. Yang, M. Mahmoud, N. Aqab, and L. Lin, "Bimorph pMUT with dual electrodes," Proceedings of the *IEEE International Conference on Micro Electro Mechanical Systems* (MEMS), vol. 2015-February, no. February, pp. 928–931,

- Feb. 2015.
- [11] S. Akhbari, F. Sammoura, S. Shelton, C. Yang, D. Horsley, and L. Lin, "Highly responsive curved aluminum nitride PMUT," Proceedings of the IEEE International Conference on Micro Electro Mechanical Systems (MEMS), pp. 124–127, 2014.
- [12] S. Akhbari, F. Sammoura, C. Yang, A. Heidari, D. Horsley, and L. Lin, "Self-curved diaphragms by stress engineering for highly responsive pMUT," in 28th IEEE International Conference on Micro Electro Mechanical Systems (MEMS), 2015, pp. 837–840.
- [13] C. Huang, S. P. Khandare, S. R. Kothapalli, and S. Tadigadapa, "Characterization of Curved Piezoelectric Micromachined Ultrasound Transducers (pMUTs) Fabricated by Chip-Scale Glass Blowing Technique," *IEEE Sens Lett*, 2023.
- [14] G. H. Feng, C. C. Sharp, Q. F. Zhou, W. Pang, E. S. Kim, and K. K. Shung, "Fabrication of MEMS ZnO dome-shaped-diaphragm transducers for high-frequency ultrasonic imaging," *Journal of Micromechanics and Microengineering*, vol. 15, no. 3, p. 586, Jan. 2005.
- [15] A. Hajati et al., "Three-dimensional micro electromechanical system piezoelectric ultrasound transducer," *Appl Phys Lett*, vol. 101, no. 25, 2012.
- [16] L. Song, S. Glinsek, and E. Defay, "Toward low-temperature processing of lead zirconate titanate thin films: Advances, strategies, and applications," *Appl Phys Rev*, vol. 8, no. 4, p. 41315, Dec. 2021.
- [17] H. Takeuchi, A. Wung, X. Sun, R. T. Howe, and T.-J. King, "Thermal budget limits of quarter-micrometer foundry CMOS for post-processing MEMS devices," *IEEE Trans Electron Devices*, vol. 52, no. 9, pp. 2081– 2086, 2005.
- [18] F. Sammoura, S. Akhbari, and L. Lin, "An analytical solution for curved piezoelectric micromachined ultrasonic transducers with spherically shaped diaphragms," *IEEE Trans Ultrason Ferroelectr Freq Control*, vol. 61, no. 9, pp. 1533–1544, 2014.
- [19] X. Jiang et al., "Monolithic ultrasound fingerprint sensor," *Microsyst Nanoeng*, vol. 3, no. 1, pp. 1–8, 2017.
- [20] Q. Wang, Y. Lu, S. Mishin, Y. Oshmyansky, and D. A. Horsley, "Design, fabrication, and characterization of scandium aluminum nitride-based piezoelectric micromachined ultrasonic transducers," *Journal of microelectromechanical systems*, vol. 26, no. 5, pp. 1132–1139, 2017.
- [21] Y. Lu et al., "Ultrasonic fingerprint sensor using a piezoelectric micromachined ultrasonic transducer array integrated with complementary metal oxide semiconductor electronics," *Appl Phys Lett*, vol. 106, no. 26, 2015.
- [22] Y. Lu, A. Heidari, and D. A. Horsley, "A high fill-factor annular array of high frequency piezoelectric micromachined ultrasonic transducers," *Journal of Microelectromechanical Systems*, vol. 24, no. 4, pp. 904– 913, 2014.
- [23] J. Lee et al., "A MEMS ultrasound stimulation system for modulation of neural circuits with high spatial resolution in vitro," *Microsyst Nanoeng*, vol. 5, no. 1, Dec. 2019.

#### CONTACT

- S. Khandare; smk7102@psu.edu
- C. Huang; huang.chic@northeastern.edu
- S. R. Kothapalli; srkothapalli@psu.edu
- S. Tadigadapa; srinivas@northeastern.edu